

## Calculations and measurements of wire and/or split-ring negative index media

F. J. Rachford, D. L. Smith, P. F. Loschialpo, and D. W. Forester

*Naval Research Laboratory, Washington, DC 20375*

(Received 19 October 2001; published 24 September 2002)

Broadband calculations (70 MHz–20 GHz) and measurements (2–15 GHz) were performed on planar stacks of two-dimensional double-split rings arrays interspersed with arrays of thin wires. Recent work on similar composite structures infers a negative index of refraction ( $n < 0$ ) over a narrow frequency range. We have performed finite-difference time-domain (FDTD) calculations on various combinations of ring geometries, wire arrays, and stack spacings. Excellent agreement was obtained between FDTD simulations and our measured transmission spectra. Examining the FDTD time progression of fields we find regions of both negative and positive indices as well as an inverse Doppler effect.

DOI: 10.1103/PhysRevE.66.036613

PACS number(s): 41.20.Jb, 42.70.Qs, 78.20.Ci, 77.22.Ch

### I. INTRODUCTION

Smith *et al.* [1–6] were the first to experimentally explore the hypothesis of Veselago [7] that if a negative permeability and negative permittivity material existed, one would have a negative index of refraction and would observe unusual behavior, such as an inverse Snell's law, an inverse Doppler effect, and backwardly propagating Cherenkov radiation. Smith *et al.* performed microwave transmission measurements combining two artificial media devised by Pendry; a conducting wire array [8–10] to reduce the plasma frequency to the microwave region and a double-split-ring resonator array [11] to provide a sharp narrow band negative permeability at a frequency band above the resonator resonance. The Pendry wire array plasma frequency is given by

$$f_p = \frac{c}{a \sqrt{2\pi \ln\left(\frac{a}{r}\right)}}, \quad (1)$$

where  $a$  is the wire lattice spacing and  $r$  is the wire radius. The double-split-ring resonance frequency is given by

$$f_o = \frac{c}{2\pi} \sqrt{\frac{3l}{\pi \epsilon r^3 \ln\left(\frac{2w}{d}\right)}}, \quad (2)$$

with  $l$  being the ring layer spacing,  $w$  the width of the rings,  $d$  is the gap width between inner and outer rings,  $r$  is the inner ring radius,  $\epsilon$  is the permittivity of the inter-ring gap, and  $c$  is the velocity of light. In Smith's [1] first realization of the wire/split-ring (WSR) medium the three-dimensional orthogonally interpenetrating Pendry wire array is replaced by a monodirectional square lattice array of wires. As long as the microwave radiation transmitted through this wire assembly is confined to propagation in the plane normal to the wire axis with electric polarization along the wire axis there will be a plasma resonance and the plasma frequency should be given by Eq. (1). Smith's split-ring structures were first created as stacked planar square arrays and later as two orthogonal stacked arrays. The wire axes were structured to lie parallel to the split ring array plane. The combined WSR stacks

were confined in a parallel plate transmission line and measurements were limited to a small portion of a waveguide band. They reported negative index for a narrow transmission peak identified with the split-ring resonance in their composite.

In the current work we have sought to extend these results through broadband (2–15 GHz) measurements and broadband (70 MHz–20 GHz) finite-difference time-domain (FDTD) simulations. We constructed and modeled physically large WSR stacks. In addition, we simulated and measured split-ring-only and wire-only arrays to further understand the transmission properties of our ring/wire composites. Our objective was to investigate sharp transmission peaks associated with split-ring resonances for negative index behavior and to measure and compute transmission in these composite structures over a wide range of wavelength scales above and below the reduced plasma and ring resonance frequencies. Our broadband simulations and measurements show a complex, rich set of spectral features reminiscent of band gap or frequency selective surface phenomena. Noting good agreement of our measurements with the simulated transmission of our composite structures, we then studied the FDTD wave propagation in the WSR medium and then find negative index and inverse Doppler shift associated with some of the observed transmission peaks.

### II. SIMULATIONS AND MEASUREMENTS

We synthesized, measured, and computer modeled thin wire arrays, resonant ring structures, and the combination of these as WSR composites. The wire arrays were constructed using 36- $\mu\text{m}$ -diameter copper wires spaced at an interval of 0.32 cm and fixed to high-density polyethylene (HDPE) substrates. The substrates are 0.16 cm thick and are stacked to achieve interlayer spacing of 0.32 cm from wire to wire or split ring to split ring with 0.16-cm spacing between wires and rings for the WSR structure.

The square resonant ring structure modeled and synthesized is shown in Fig. 1. The copper ring pattern is roughly 1  $\mu\text{m}$  thick on a 0.015-cm polyimide substrate. The outer square side length is 0.99 cm while the inner square side length is 0.55 cm. The width of the etched copper segments is 0.10 cm. The gap spacing between inner and outer rings is

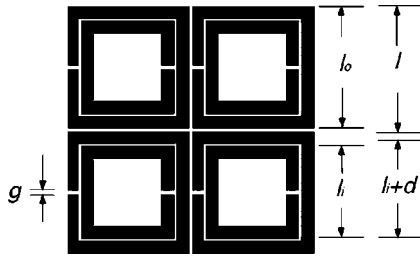


FIG. 1. Square double ring geometry. Lattice constant  $l = 1.04$  cm, ring's outer dimensions  $l_o = 0.99$  cm, etched linewidth 1 mm, inner ring's outer dimensions  $l_i = 0.75$  cm, inter-ring gap of 0.2 mm, and ring gap  $g = 0.04$  cm.

$d = 0.02$  cm and square planar array lattice constant is 1.04 cm. Over 100 planar arrays with  $9 \times 40$  elements were stacked, aligned, and spaced 0.32 cm apart by HDPE. Measurements were made with the  $H_{rf}$  vector perpendicular to the loops and the  $E_{rf}$  vector aligned along the wire axes.

Although the individual planar ring arrays and planar wire arrays were accurately registered with each other from layer to layer, the wire array spacing and the ring array period were incommensurate. In the FDTD simulations a commensurate spacing was used. This was achieved by increasing the wire in-plane spacing by 3%. This small correction was considered acceptable in light of other experimental uncertainties in the assembly. Subsequent analysis has shown that the registration has little effect on the spectral features.

The sample stacks were measured in a microwave quasi-optical, focused beam apparatus. In the sample region the microwave energy is compressed to a diffraction limited Gaussian profile. Both broadband and waveguide feeds were used to launch and receive the transmitted microwave energy. The greatest dynamic range and accuracy occurred with the waveguide feeds since the stacks had a very large polarization anisotropy and the waveguide allowed greater accuracy in aligning the linearly polarized microwave radiation with the layered ring/wire structure.

### III. RESULTS

Transmission through the HDPE alone without rings or wires resulted in a frequency independent measured permittivity of  $\epsilon = 2.35 + 0.014i$  in agreement with expectations for this material. Inverting the complex transmission coefficient for the 0.32-cm wire array on HDPE with 0.32-cm layer spacing we obtain the complex permittivity shown in Fig. 2. The details will be published elsewhere. The real part of the measured permittivity (bold solid curve) crosses the zero axis at approximately 12 GHz. The bold dashed curve is the measured imaginary part of the permittivity. The fine solid and dashed curves are the calculated values of the real and imaginary permittivities using the Pendry model. The real permittivity is in excellent agreement with the simple Pendry model. The measured imaginary permittivity is greater than expected below the effective plasma frequency.

In Fig. 3(a) we compare the FDTD computed transmission with the measured transmission in dB referenced to free space for a stack of square resonant rings only on HDPE.

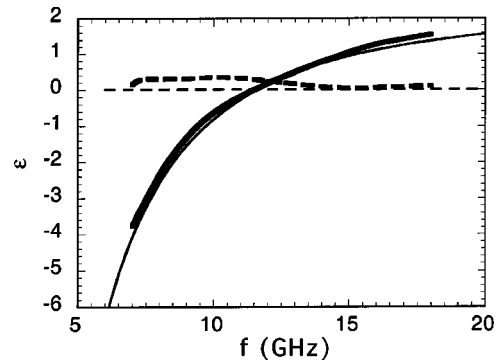


FIG. 2. Measured permittivity of a 1.27-cm-thick wire array in HDPE. The square lattice of wires has lattice constant 0.32 cm. The bold solid curve is  $\text{Re}(\epsilon)$  and the bold dashed curve is  $\text{Im}(\epsilon)$ . The fine solid and dashed curves are the computed values using the Pendry model with the imaginary permittivity indistinguishable from 0 in this plot.

The ring layers are spaced 0.32 cm apart and no wires are included in the stack. The measured data (red curve) were taken in three waveguide frequency bands and closely match the FDTD simulation (blue curve). In Fig. 3(b) we have inserted the wires so that the wire arrays are spaced 0.16 cm

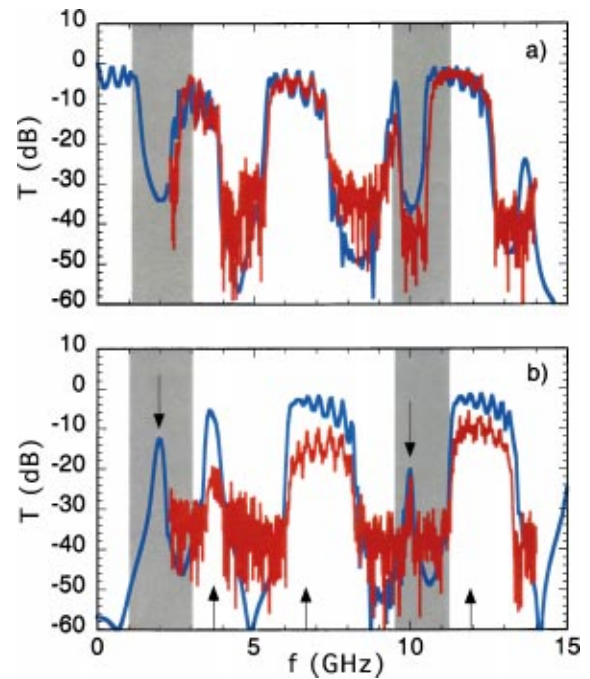


FIG. 3. (Color) Calculated (blue) and measured (red) transmission spectra for stacks of square Pendry ring arrays on HDPE (a) and ring and wire arrays (b). The ring arrays are stacked 0.32 cm apart, while the alternating ring and wire arrays are stacked 0.16 cm from each other. Frequency regions near 2 and 10 GHz are highlighted since they appear to behave as expected from simple theory; i.e., an absorption band in the ring-only structure yields transmission peak in the combined WSR structure. The arrows indicate frequencies at which detailed FDTD simulations were run following the time dependence of the wave propagation in the split ring alone and WSR composites.

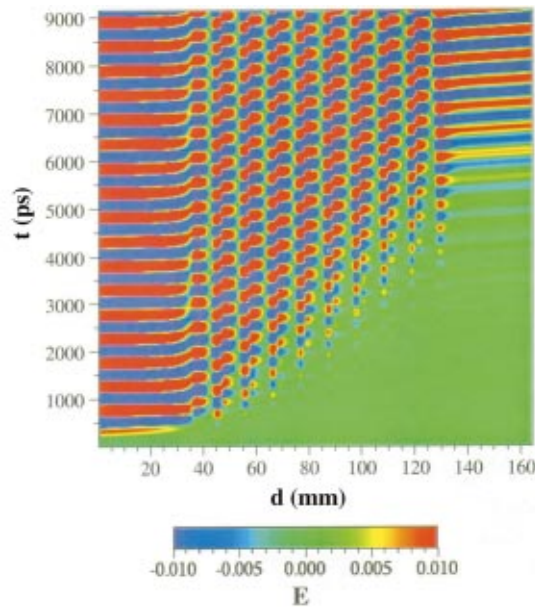


FIG. 4. (Color) Propagation of 1.96-GHz microwave radiation through our ring/wire composite media. A plane wave is assumed to enter from the left. Time is plotted on the vertical axis while distance is plotted on the horizontal axis. From 0 to 35 mm the wave is in free space. The wave enters the ring/wire medium with  $E$ -field polarization along the direction of the wires. It takes several cycles before the resonant response of the medium settles into a steady state. At 129 mm, the radiation exits from the medium. The color scale is saturated to highlight the position of successive  $E$ -field crests and troughs. In this case resonances at the ring locations are pronounced and the apparent index of refraction is ambiguous:  $n = +11.8$  is for rising phase slope and  $n = -3.6$  for decreasing phase slope.

below and above the rings in the stack layers. Once again the FDTD simulation reproduces the main features of the measured data. Some variation is seen in the amplitude of the transmission bands but these bands and even most of the small Fresnell interference peaks are accurately placed in frequency. The wires also introduce some transmission loss increasing with decreasing frequency, which is not modeled well in either the FDTD or simple Pendry predictions. This is consistent with the measured imaginary part of the permittivity of the wire array (Fig. 2), which is also larger than expected. The modeling assumed pure copper conductivity, however, we made no attempt to improve the surface condition of our wires.

According to first-order analysis the ring-only transmission spectra should display transmission nulls at the split-ring resonator resonances. Substituting the split-ring parameters into Eq. (2) we expect the fundamental split-ring resonance to occur at 7 GHz. Our FDTD calculations show split-ring resonances at 2, 5, and 10 GHz. Upon introducing the wire arrays transmission peaks should appear in the permeability resonance transmission nulls below the effective plasma frequency (12 GHz). The WSR transmission peaks at 1.96 GHz and 9.98 GHz occur in split-ring only transmission nulls and are suggestive of the results expected from the

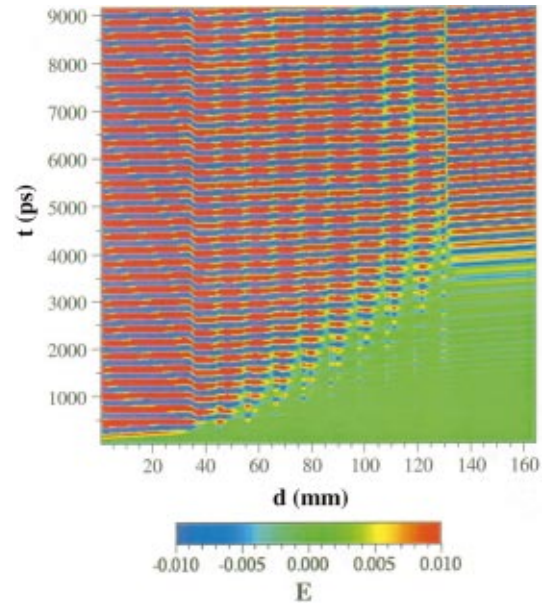


FIG. 5. (Color) Propagation of 6.93-GHz microwave radiation through our ring/wire composite media. The phase propagation is more continuous and the apparent index of refraction is  $n = +1.0$ .

Pendry effective medium model. [See shaded regions in Figs. 3(a) and 3(b).]

Since the FDTD simulation appears to correctly model the transmission data, we now investigate wave propagation inside the stack by querying the FDTD model at positions along the direction of wave propagation as a function of time at several microwave frequencies. Figures 4–6 show the  $E$  field propagation through the sample as a function of time at

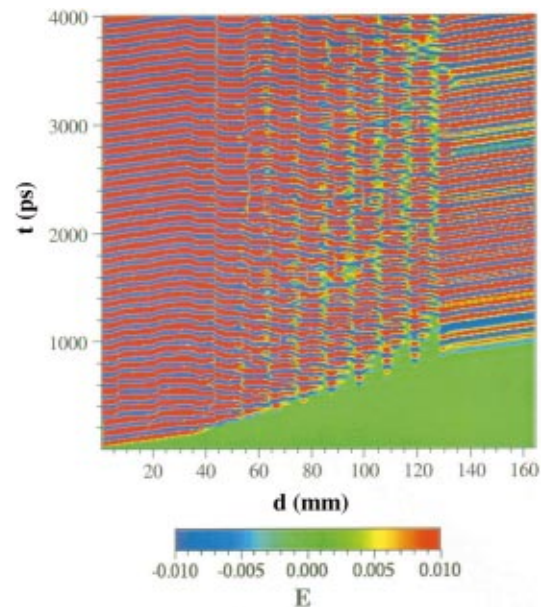


FIG. 6. (Color) Propagation of 9.98 GHz microwave radiation through our ring/wire composite media. The apparent index of refraction is  $n = -1.4$ . An observer well inside of the WSR medium traveling away from the microwave source would initially experience an inverse Doppler shift; i.e., an increase in frequency in encountering wave crests.

various transmission peak frequencies. The saturated color scale is proportional to the instantaneous field amplitude. At 1.96 GHz (Fig. 4) there are strong resonances at the ring positions. Tracing the slope of the  $E$  field maxima (red) is ambiguous. One could determine the index of refraction to be either  $+11.8$  or  $-3.6$ . This frequency corresponds to the lowest frequency peak in Fig. 3(b). Sampling the wave propagation at the broad transmission band between 6 and 8 GHz [see arrow in Fig. 3(b)], we find that the localized resonances are less pronounced and the effective index is approximately 1.0 (see Fig. 5). In Fig. 6 the phase propagation is dramatically different. This frequency corresponds to the transmission peak at 9.98 GHz [see arrow in Fig. 3(b)]. Initially, the wave enters the material (40 mm), initiating resonant scattering in the ring structures. Once a steady state is established (55 mm), we note that the slope of the crests and valleys is negative. Comparing the wavelengths inside and outside of the material we find an effective index of refraction  $n = -1.4$ . In Table I we list frequencies and estimated refractive indices for the ring/wire stack at selected frequencies indicated by the arrows in Fig. 3. This table also indicates an effective negative index for the broad transmission peak at 11.9 GHz. A second negative index peak is unexpected, especially above 11.5 GHz where the permittivity of the wire-only array becomes positive (see Fig. 2).

#### IV. DISCUSSION

The measured and calculated transmission spectra for the stacks with and without wires are substantially different from those expected from superimposition of wire permittivity and ring permeability of the simple Pendry effective medium theory. The measurements and simulations show a complex series of bandpass and bandstop regions along with a sharp spectral feature at 10 GHz similar to that of Smith *et al.* This feature displays negative index, “left-handed” behavior in the FDTD analysis. The similar peak at 1.96 GHz possibly may be due to negative index, however, at this low frequency, propagation of the wave front in our 10-cm-thick WSR structure was ambiguous (see Fig. 4). The presence of positive index transmission peaks at lower frequencies challenges the simple theory since the real part of the permittivity should be strongly negative a few GHz below the measured plasma frequency. In particular, negative index at 11.9 GHz is unexpected. More detailed theoretical analysis is needed for these complex interacting structures to fully understand the observed phenomena. An interplay of electric and magnetic structural resonances and photonic band gap edge effects [12] are probably responsible for our broadband observations.

We note in passing that the reversal of the Doppler shift in left-handed materials is manifested in the field propagation plot in Fig. 6. A stationary observer represented by a vertical line would measure 100 ps between adjacent crests. Yet an observer traveling away from the source, represented by a line with a positive slope, would measure a smaller time interval between the crests (blue shift). This is the opposite

TABLE I. Frequency of FDTD calculation and the effective index of refraction for microwave propagation in our ring/wire stack. Refer to arrows in Fig. 3(b) for the position of these frequencies in the transmission spectrum.

$f$ (GHz)	$n$
1.96	$-3.6$ or $+11.8$
3.57	$+1.6$
6.93	$1.0$
9.98	$-1.4$
11.90	$-0.9$

of what occurs in a conventional positive index material.

We are continuing simulation, construction, and measurement of ring/wire composites. Interesting results on ring-only composites and on apparent focusing in transmission of divergent microwave radiation through the composites will be published elsewhere.

#### V. CONCLUSION

We have performed FDTD simulations, constructed, and measured stacks of arrays of Pendry double rings and wires under illumination by normally incident, linearly polarized microwave radiation. Although the superposition of simple Pendry models does not appear to be correct for the entire bandwidth of our investigation, the complex transmission structure of transmission peaks and bands can be accurately calculated by finite-difference time-domain simulations. An examination of the spectral peaks for rings alone and full wire/ring stacks displays some features that are consistent with the Pendry theory; i.e., transmission notches for rings alone transforming to transmission peaks in the combined structures. However, the broadband transmission spectra are much more complex than anticipated. We investigated the time dependent microwave fields as a function of position through the stack, and note apparent negative index behavior at select frequencies in the composite material. In contrast to the simple split-ring theory, our FDTD simulations (not shown here) reveal that none of the spectral peaks move in frequency as the gap spacing between the rings is varied. Additionally, we directly inverted the complex transmission coefficient for the case of a wire array and find a composite negative permittivity in agreement with the Pendry model. Previous work has suggested that permittivity and permeability may alternately be negative in successively higher photonic band gaps [12]. The negative index transmission regions observed in this work may involve interplay between conventional resonances and photonic band gap effects.

#### ACKNOWLEDGMENTS

This work was supported by DARPA. The authors gratefully acknowledge the technical support provided by Debra Dutko of SFA, inc.

- [1] D.R. Smith, W.J. Padilla, D.C. Vier, S.C. Nemat-Nasser, and S. Schultz, *Phys. Rev. Lett.* **84**, 4184 (2000).
- [2] D.R. Smith, D.C. Vier, N. Kroll, and S. Schultz, *Appl. Phys. Lett.* **77**, 2246 (2000).
- [3] D.R. Smith and N. Kroll, *Phys. Rev. Lett.* **85**, 2933 (2000).
- [4] R.A. Shelby, D.R. Smith, and S. Schultz, *Science* **77**, 292 (2001).
- [5] P. Weiss, *Sci. News* **157**, 199 (2000).
- [6] R. Fitzgerald, *Physics Today* **54**(5), 17 (2001).
- [7] V.G. Veselago, *Sov. Phys. Usp.* **10**, 509 (1968).
- [8] J.B. Pendry, A.J. Holden, W.J. Stewart, and I. Youngs, *Phys. Rev. Lett.* **76**, 4773 (1996).
- [9] J.B. Pendry, A.J. Holden, D.J. Robbins, and W.J. Stewart, *J. Phys.: Condens. Matter* **10**, 4785 (1998).
- [10] J.B. Pendry, A.J. Holden, D.J. Robbins, and W.J. Stewart, *IEEE Trans. Microwave Theory Tech.* **47**, 2075 (1999).
- [11] J.B. Pendry, *Phys. Rev. Lett.* **85**, 3966 (2000).
- [12] C.A. Kyriazidou, H.F. Contopanagos, W.M. Merrill, and N.G. Alexopoulos, *IEEE AP-S Int. Symp. Dig.* **3**, 1912 (1999). Calculations confirmed by authors of this paper.